Integral Equation Method for Subsonic Flow Past Airfoils in Ventilated Wind Tunnels

M. MOKRY*
National Research Council of Canada, Ottawa, Ontario, Canada

The method of contour distribution of sources and vortices, used to calculate potential flows about two-dimensional airfoils in free air, is extended to flows around airfoils under the constraint of ventilated wind tunnel walls. Based on the concept of fundamental solutions, the source and vortex singularities are modified to satisfy the boundary conditions at the walls. The application of the airfoil boundary condition reduces the problem to a Fredholm integral equation of the second kind for the source density function. The numerical solutions obtained by a finite element technique are in good agreement with experimental results.

I. Introduction

A LARGE part of established wall interference theory is based on the simplifying assumption that the wall effects can be evaluated from an estimated far flowfield of the model, considering only the wind tunnel wall boundary condition. The result is interpreted in terms of modifications to the freestream. If the model is small enough, these can be expressed as corrections to the direction and speed of the stream, constant over the model (the angle of attack and Mach number corrections). If the model has appreciable length, a more refined interpretation, involving the streamline curvature and buoyancy (pressure gradient) effects, is required. The model boundary condition enters the problem only in the final stage, if there is a need to evaluate the wall effects in terms of model quantities, such as the surface pressure distribution, aerodynamic forces, moments, etc. A comprehensive account of this approach, its applicability and limitations is given in Ref. 1.

It is perhaps worth emphasizing that the above concept proves very useful, giving valid engineering approximations in a variety of practical applications. On the other hand, there is no doubt that a correct approach to the wind tunnel problem should be based on solutions which satisfy both the wall and model boundary conditions. The distinct feature of such an approach is that model quantities, influenced by the walls, are evaluated directly, whereas the corresponding corrections to the freestream cannot be obtained explicitly. Comparisons with free air calculations present no great problems in principle, but it may well be impossible to interpret the wind tunnel calculations in terms of simple corrections to the freestream, as we know them.

In this paper a method is outlined to calculate two-dimensional incompressible flow past airfoils in a ventilated wind tunnel. By utilizing the simple compressibility transformations, it is extended to subsonic linearized flows. The mathematical formulation relates to the Poincaré boundary value problem,[2] first used in the theory of tides. Using the concept of fundamental solutions and surface layers, the problem is further solved along the lines of the source distribution method.[3,4] Conceptually, the approach is similar to that used for airfoils in a cascade or hydrofoils under a free surface. As in Ref. 4, an auxiliary distribution of vortices is used to provide the solution with a circulation. The influence functions, which correspond to complex disturbance velocities due to a point source and a point vortex between two porous infinite walls, are evaluated in closed form[5] using the method of images. The application of the airfoil boundary condition leads to a Fredholm integral equation of the second kind for the source density function. The integral equation formulation was selected largely because of its compactness. It is assumed that in the process of computation, the continuous mathematical model will be discretized by finite elements as is the case in Refs. 3 and 4. It is noted that an alternative approach can be developed by adapting the vortex distribution method[6-8] using virtually the same influence functions.

As far as the motivation of the present work is concerned, it is realized that one mostly thinks of ventilated wind tunnels in connection with the transonic or supersonic testing because of their ability to attenuate the choking and wave reflection phenomena. However, our frequent interest in landing and taking-off characteristics requires some low-speed testing as well, and then, in order to obtain consistent wind tunnel data when going down to low speeds, the wind tunnel walls are usually left unchanged. In any case, the solid walls, which probably are well suited for two-dimensional low-speed tests, are treated by the present method (as a special case) far more efficiently than it is possible with the usual modeling by an infinite cascade of mirror image airfoils. Since the incompressible flow version of the present method is exact in its formulation, the results obtained may also serve as low-speed test cases for various numerical methods of wind tunnel flow calculation.

II. Formulation of the Problem

Two-dimensional wind tunnel flows, whose disturbance velocity potential ϕ is governed by the Laplace equation

$$\partial^2\phi/\partial x^2+\partial^2\phi/\partial y^2=0 \qquad (1)$$

can be studied in connection with the Poincaré problem.[2] Let D_F be a region (open, connected set) and let C_F be its topological boundary. Denoting by $\mathscr{C}^m$ the set of m-times continuously differentiable functions, it is required to find a function $\phi\in\mathscr{C}^2(D_F)$ and $\phi\in\mathscr{C}^1(D_F\cup C_F)$ satisfying Eq. (1) in D_F and

$$a(s)\partial\phi/\partial n+b(s)\partial\phi/\partial s+c(s)\phi=q(s) \quad \text{on} \quad C_F \qquad (2)$$

Here $a(s)$, $b(s)$, $c(s)$, and $q(s)$ are real functions given on C_F, s is the arc length coordinate, and n the normal to C_F. The existence-uniqueness conditions of the above problem are discussed in Ref. 9.

In the case under consideration, Fig. 1, D_F is a multiply connected flow region bounded by nonintersecting contours

Presented as Paper 74-83 at the AIAA 12th Aerospace Sciences Meeting, Washington, D.C., January 30–February 1, 1974; submitted February 13, 1974; revision received June 19, 1974.

Index categories: Subsonic and Transonic Flow; Nozzle and Channel Flow; Aircraft Aerodynamics (Including Component Aerodynamics); Aircraft Testing (Including Component Wind Tunnel Testing).

* Associate Research Officer, High-Speed Aerodynamics Laboratory. Member AIAA.

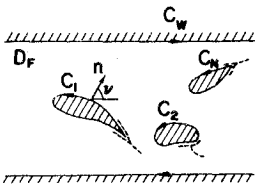

Fig. 1 Flow region D_F.

C_W (wind tunnel boundary) and $C_1, C_2, \ldots, C_N$ (boundaries of N airfoils). The boundary C_W comprises two parallel straight lines, representing infinite walls. The closed contours $C_1, C_2, \ldots, C_N$ are assumed to be smooth, with a possible exception of branch points of dividing streamlines (leading or trailing edges). In any case, the N trailing edge points, one per each contour $C_1, C_2, \ldots, C_N$ are supposed to be specified.[10]

We denote by C the union of airfoil boundaries $C = C_1 \cup C_2 \cup \ldots \cup C_N$ and by C_F the flow boundary $C_F = C_W \cup C$. The positive direction on C_F is assumed such that the flow region D_F lies to the right of C_F (i.e. counterclockwise on C and clockwise on C_W). The normal n is oriented to point into D_F, so that it is the outward normal to C.

The boundary condition on C_W is assumed to be homogeneous:

$$a(s)\,\partial\phi/\partial n + b(s)\,\partial\phi/\partial s + c(s)\,\phi = 0 \tag{3}$$

that is, the right-hand side $q(s) = 0$. Depending on the kind of the walls, we may deal with the following particular cases of Eq. (3): 1) closed (solid) wall, $\partial\phi/\partial n = 0$; 2) open jet boundary, $\partial\phi/\partial s = 0$; 3) porous or perforated wall, $\partial\phi/\partial n \mp P(s)\,\partial\phi/\partial s = 0$, $P(s) > 0$; 4) slotted wall, $-K(s)\,\partial\phi/\partial n + \phi = 0$, $K(s) > 0$.

In cases 3 and 4, the boundary conditions are representative of the walls only in the integral sense, neglecting the variations of flow quantities between the open and closed portions of the walls. The boundary condition for a porous wall, upon interpreting $\partial\phi/\partial s$ in terms of a pressure disturbance, is identified as the Darcy law for porous media. The minus sign refers to the wall oriented downstream (upper wall in Fig. 1), and the plus sign to the wall oriented upstream (lower wall).

$P(s)$ is the porosity parameter, which physically relates the pressure difference across the wall to flow through the wall. Because of the complicated nature of flow through the wall, $P(s)$ has to be determined experimentally. It may vary between 0 for closed walls and ∞ for open jet.

The slot parameter $K(s)$ derived in Ref. 11 on the basis of inviscid flow at the slots, appears to be a simple function of the slot width and the distance between slots. However, the experimental investigations of Ref. 12 indicate that in practice, the slotted walls are better described by the porous wall theory, possibly due to large viscous effects.

The flow is supposed to be tangent to the airfoil boundary C. Assuming the freestream velocity vector to be of unit magnitude and oriented along the positive x-axis, and denoting by $\nu = \nu(s)$ the angle between the normal n and the x-axis, we obtain the inhomogeneous boundary condition

$$\partial\phi/\partial n = -\cos\nu \qquad \text{on} \qquad C \tag{4}$$

The problem is solved using the concept of fundamental solutions and surface layers. The fundamental solution g_σ of the Laplace operator with a pole at x_0, y_0 satisfies the differential equation

$$\partial^2 g_\sigma/\partial x^2 + \partial^2 g_\sigma/\partial y^2 = \delta(x-x_0)\delta(y-y_0)$$

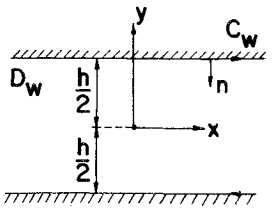

Fig. 2 Wind tunnel region D_w.

where δ denotes the Dirac delta function. In the region D_W bounded by C_W, Fig. 2, g_σ takes the form

$$g_\sigma(x,y;\,x_0,y_0) = (2\pi)^{-1}\log\left[(x-x_0)^2+(y-y_0)^2\right]^{1/2} + h_\sigma(x,y;\,x_0,y_0) \tag{5}$$

where h_σ is an arbitrary harmonic function in D_W. Assuming that it is possible to construct h_σ in such a way that g_σ satisfies

$$a(s)\,\partial g_\sigma/\partial n + b(s)\,\partial g_\sigma/\partial s + c(s) g_\sigma = 0 \qquad \text{on} \qquad C_W \tag{6}$$

then a solution ϕ obtained by linear superposition of g_σ evidently satisfies Eq. (3). Since Eq. (5) describes the potential due to a unit source, unable to generate circulation, we consider additional use of the potential due to a unit vortex

$$g_\gamma(x,y;\,x_0,y_0) = -(2\pi)^{-1}\operatorname{atan}\left[(y-y_0)/(x-x_0)\right] + h_\gamma(x,y;\,x_0,y_0) \tag{7}$$

The form of Eq. (7) is accepted on the grounds that the harmonic conjugate of g_γ is a fundamental solution. By the same reasoning we require

$$a(s)\,\partial g_\gamma/\partial n + b(s)\,\partial g_\gamma/\partial s + c(s) g_\gamma = 0 \qquad \text{on} \qquad C_W \tag{8}$$

In analogy with free air calculations[4] suppose that g_σ and g_γ are distributed on C with the line densities σ and γ respectively. By the principle of linear superposition, the potential due to the entire distribution is

$$\phi(x,y) = \int_C \left[\sigma(x_0,y_0) g_\sigma(x,y;\,x_0,y_0) + \gamma(x_0,y_0) g_\gamma(x,y;\,x_0,y_0)\right] ds_0 \tag{9}$$

where

$$ds_0 = \left[(dx_0)^2+(dy_0)^2\right]^{1/2} \tag{10}$$

is the contour element of C. The subscript 0 refers to the dummy variables of integration.

We note that of the entire flow boundary C_F, the integral, Eq. (9), is taken only over C, where the corresponding boundary condition, Eq. (4), is inhomogeneous. The homogenity of the wind tunnel boundary condition in Eq. (3) implies that the flow across C_W is continuous, and presumably no singularities should be used there.

From Eqs. (6) and (8) it follows that the potential of Eq. (9) automatically satisfies Eq. (3) on C_W. We then assume that it is possible to adjust the density functions σ and γ in such a way that the inhomogeneous boundary condition on C [Eq. (4)] together with the Kutta-Joukowski condition, are also satisfied.

III. Reduction of the Problem to an Integral Equation

The detailed treatment of the problem is greatly simplified by employing complex variables

$$z = x + iy \tag{11}$$

$$z_0 = x_0 + iy_0 \tag{12}$$

and the complex disturbance velocity

$$w = \partial\phi/\partial x - i\,\partial\phi/\partial y \tag{13}$$

By Eq. (9) we find

$$w(z) = \int_C \left[\sigma(z_0) G_\sigma(z;\,z_0) + \gamma(z_0) G_\gamma(z;\,z_0)\right] ds_0 \tag{14}$$

where $\sigma(z_0)$ and $\gamma(z_0)$ denote the functional values of the density functions σ and γ at x_0, y_0.

Using Eqs. (5) and (7), the influence functions

$$G_\sigma = \partial g_\sigma/\partial x - i\,\partial g_\sigma/\partial y$$
$$G_\gamma = \partial g_\gamma/\partial x - i\,\partial g_\gamma/\partial y \tag{15}$$

can be evaluated as

$$G_\sigma(z;\,z_0) = \left[2\pi(z-z_0)\right]^{-1} + H_\sigma(z;\,z_0)$$
$$G_\gamma(z;\,z_0) = i\left[2\pi(z-z_0)\right]^{-1} + H_\gamma(z;\,z_0) \tag{16}$$

where

$$H_\sigma = \partial h_\sigma/dx - i\,\partial h_\sigma/\partial y$$
$$H_\gamma = \partial h_\gamma/\partial x - i\,\partial h_\gamma/\partial y \tag{17}$$

are analytic in D_w.

The contour length element ds_0, Eq. (10), can be expressed as

$$ds_0 = -i\exp(-iv_0)\,dz_0 \tag{18}$$

where v_0 is the angle between the outward normal to ds_0 and the x-axis.

Assuming that the function $\sigma+i\gamma$ satisfies the Hölder condition[9] everywhere on C (in a weak sense near cusps), we obtain from Eqs. (14) and (18) the limiting value of $w(z)$ as z approaches a smooth segment of C along any path entirely in D_F (Plemelj formula):

$$w(z) = \oint_C [\sigma(z_0)G_\sigma(z;\,z_0)+\gamma(z_0)G_\gamma(z;\,z_0)]\,ds_0 + [\sigma(z)+i\gamma(z)]\exp(-iv)/2, \qquad z\in C \tag{19}$$

The integral denoted by the symbol $\oint$ is the Cauchy principal value. It can be shown that $w(z)$ is continuous in $D_F \cup C_F$.

The airfoil boundary condition, Eq. (4), is expressed in terms of w as follows:

$$Re\,[w\exp(iv)] = -\cos v \tag{20}$$

Substituting Eq. (19) in Eq. (20) we obtain a Fredholm integral equation of the second kind for the source density function σ:

$$\sigma(z)/2+\oint_C \sigma(z_0)K(z;\,z_0)\,ds_0 = -\cos v - Re\,[\exp(iv)\oint_C \gamma(z_0)G_\gamma(z;\,z_0)\,ds_0] \tag{21}$$

where

$$K(z;\,z_0) = Re\,[\exp(iv)G_\sigma(z;\,z_0)] \tag{22}$$

We assume the solution in the form

$$\sigma(z) = \sigma_0(z)+\sum_{k=1}^{N} a_k\sigma_k(z), \qquad a_k \text{ real} \tag{23}$$

where $\sigma_0(z)$ is the solution of

$$\sigma_0(z)/2+\oint_C \sigma_0(z_0)K(z;\,z_0)\,ds_0 = -\cos v \tag{24}$$

and $\sigma_k(z)$ is the solution of

$$\sigma_k(z)/2+\oint_C \sigma_k(z_0)K(z;\,z_0)\,ds_0 = -Re\,[\exp(iv)\oint_{C_k} \gamma_k(z_0)G_\gamma(z;\,z_0)\,ds_0], \qquad k=1,\ldots,N \tag{25}$$

Physically, Eqs. (24) and (25) represent the decomposition of the problem into the "uniform" and "circulatory" onset flows.[3,4] The sufficient condition for the existence of the right-hand side integral of Eq. (25) is that γ_k satisfy the Hölder condition. In order to generate nonzero circulation, we further require that $\int_{C_k}\gamma_k(z_0)\,ds_0 \neq 0$. Among some simplest choices are $\gamma_k = 1$ (used in Ref. 4) or $\gamma_k = r_k$, where r_k is the distance from the trailing edge point.

By direct substitution of Eqs. (23–25) in (21) it is found that

$$\gamma(z) = a_k\gamma_k(z), \qquad z\in C_k \tag{26}$$

The constants a_k are found from the condition of continuity of w at the trailing edge points (Kutta-Joukowski condition). This indicates that a wedge-shaped or a blunt trailing edge has to be a stagnation point, i.e.,

$$1+w = 0 \tag{27}$$

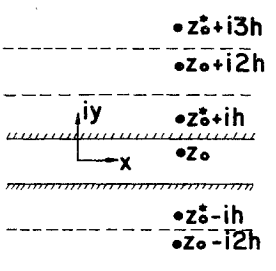

Fig. 3 Sequence of images of z_0.

whereas at a cusped trailing edge $1+w$ may be finite. The application of the Kutta-Joukowski condition to all N trailing edges leads to a system of N linear algebraic equations in N unknowns a_k. Having determined a_k, we can calculate the resultant density functions σ and γ from Eqs. (23) and (26), and evaluate the complex disturbance velocity w from Eq. (14). The Bernoulli equation can be used to obtain the corresponding pressure coefficient

$$C_p(z) = 1-|1+w(z)|^2 \tag{28}$$

IV. Influence Functions for Walls with Constant Porosity Factors

It becomes evident that the crucial part of the method is the determination of the influence functions G_σ and G_γ. Various techniques of the mathematical physics can be used for this purpose, as demonstrated in Refs. 11, 13, and 14 (Fourier transform); Ref. 15 (Laplace transform); Refs. 5, 16, and 17, (method of images); Ref. 18 (eigenfunction expansion); etc.

As an example we consider a simple case of porous or perforated walls, having constant porosity factors:

$$P(s) = \begin{cases} P_U > 0, & y = h/2 \\ P_L > 0, & y = -h/2 \end{cases}$$

where h is the wind tunnel height, Fig. 2. The assumption of different porosity factors P_U and P_L proves useful in physical situations where the upper and lower walls exhibit a different cross-flow behavior.[19]

The influence functions are derived by the method of images, which under the circumstances appears to be the least laborious approach. Using Eq. (3), case 3, and Eq. (13) we obtain the boundary condition for $w = w(z)$

$$\begin{aligned} P_U\,Re\,w - Im\,w &= 0, \qquad z = x+ih/2 \\ P_L\,Re\,w + Im\,w &= 0, \qquad z = x-ih/2 \end{aligned} \tag{29}$$

Similarly, from Eqs. (6), (8), and (15) it follows that the corresponding influence functions $G = G_\sigma(z;\,z_0)$ and $G = G_\gamma(z;\,z_0)$ are required to satisfy

$$\begin{aligned} P_U\,Re\,G - Im\,G &= 0, \qquad z = x+ih/2 \\ P_L\,Re\,G + Im\,G &= 0, \qquad z = x-ih/2 \end{aligned} \tag{30}$$

As a starting point for the construction of the influence functions, Eq. (16), the images formed by the upper wall will be examined. In the half-plane $y < h/2$, we wish to determine an analytic function $H_\sigma{}^U(z;\,z_0)$ such that

$$G_\sigma{}^U(z;\,z_0) = [2\pi(z-z_0)]^{-1}+H_\sigma{}^U(z;\,z_0) \tag{31}$$

satisfies the upper wall boundary condition

$$P_U\,Re\,G_\sigma{}^U - Im\,G_\sigma{}^U = 0, \qquad z = x+ih/2 \tag{32}$$

We assume that $H_\sigma{}^U$ has a singularity at the image point $z_0{}^*+ih$ of the source point z_0 with respect to the wall, as illustrated in Fig. 3. The asterisk denotes complex conjugation:

$$z_0{}^* = x_0 - iy_0 \tag{33}$$

Since the boundary condition [Eq. (32)] does not involve derivatives of $G_\sigma{}^U$, we deduce that an image of a simple pole

$$[2\pi(z-z_0)]^{-1}$$

will again be a simple pole

$$H_\sigma{}^U = [2\pi(z-z_0{}^*-ih)]^{-1}(a+ib) \tag{34}$$

The unknown real constants a, b are determined by substituting Eqs. (31, 34) in Eq. (32). We obtain

$$\begin{aligned} a &= (1-P_U{}^2)/(1+P_U{}^2) = \cos\pi t_U \\ b &= 2P_U/(1+P_U{}^2) = \sin\pi t_U \end{aligned}$$

where

$$t_U = (2/\pi)\,\text{atan}\,P_U, \qquad 0 < t_U < 1 \tag{35}$$

Hence

$$H_\sigma{}^U(z;\,z_0) = [2\pi(z-z_0{}^*-ih)]^{-1}\exp(i\pi t_U)$$

In a similar way we can show that a pole

$$[2\pi(z-z_0)]^{-1}(\sigma+i\gamma) \tag{36}$$

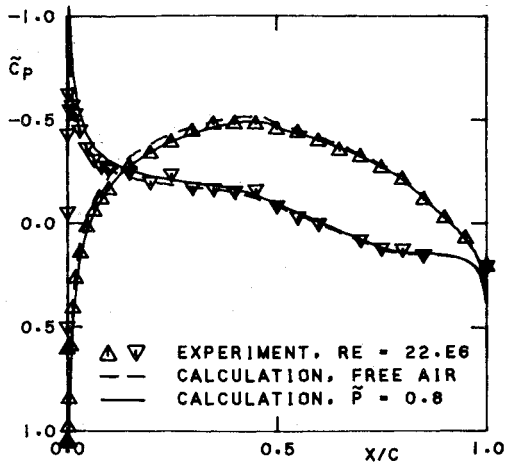

Fig. 4 NACA 64A410 airfoil, 15 in. model, $M = 0.500$, $\alpha = -1.48°$.

of the strength $\sigma + i\gamma$ has an upper wall image

$$\sigma H_\sigma{}^U + \gamma H_\gamma{}^U = [2\pi(z - z_0{}^* - ih)]^{-1}(\sigma + i\gamma)^* \exp(i\pi t_U) \quad (37)$$

and a lower wall image

$$\sigma H_\sigma{}^L + \gamma H_\gamma{}^L = [2\pi(z - z_0{}^* + ih)]^{-1}(\sigma + i\gamma)^* \exp(-i\pi t_L) \quad (38)$$

where

$$t_L = (2/\pi) \operatorname{atan} P_L, \qquad 0 < t_L < 1 \quad (39)$$

However, in the case of two walls the boundary conditions, Eq. (30), have to be satisfied simultaneously. By analogy with the formation of optical images by two parallel mirrors, the boundary effect of the walls is given by a sequence of images, located at $z_0{}^* + ih, z_0{}^* - ih, z_0 + i2h, z_0 - i2h, z_0{}^* + i3h$, and so on (see Fig. 3). The only singularity exhibited in D_w is the original pole at z_0. The singular points of H_σ and H_γ, representing the wall effects, are outside D_w as required. Using Eqs. (37) and (38) and the approach of Ref. 5, the boundary effect of the walls due to the pole of Eq. (36) can be written in terms of infinite series

$$\begin{aligned}\sigma H_\sigma + \gamma H_\gamma = {} & [2\pi(z - z_0{}^* - ih)]^{-1}(\sigma + i\gamma)^* \exp(i\pi t_U) + \\ & [2\pi(z - z_0{}^* + ih]^{-1}(\sigma + i\gamma)^* \exp(-i\pi t_L) + \\ & [2\pi(z - z_0 - i2h)]^{-1}[(\sigma + i\gamma)^* \exp(-i\pi t_L)]^* \exp(i\pi t_U) + \\ & [2\pi(z - z_0 + i2h)]^{-1}[(\sigma + i\gamma)^* \exp(i\pi t_U)]^* \exp(-i\pi t_L) + \ldots \\ & = (\sigma + i\gamma)B + (\sigma - i\gamma)E \end{aligned} \quad (40)$$

where

$$B = (2\pi)^{-1} \sum_{m=1}^{\infty} [z - z_0 - i2mh]^{-1} \exp\{i\pi m(t_U + t_L)\} + [z - z_0 + i2mh]^{-1} \exp\{-i\pi m(t_U + t_L)\} \quad (41)$$

$$E = (2\pi)^{-1} \sum_{m=1}^{\infty} [z - z_0{}^* - i(2m-1)h]^{-1} \times \exp\{i\pi[mt_U + (m-1)t_L]\} + [z - z_0{}^* + i(2m-1)h]^{-1} \times \exp\{-i\pi[(m-1)t_U + mt_L]\} \quad (42)$$

The series B and E can be summed using the relation

$$\sum_{m=1}^{\infty} (\zeta - im)^{-1} \exp(im\tau) + (\zeta + im)^{-1} \exp(-im\tau) = 2\pi \exp(\tau\zeta)/[\exp(2\pi\zeta) - 1] - \zeta^{-1}, \qquad 0 < \tau < 2\pi \quad (43)$$

following from the Fourier expansion of $\exp(\tau\zeta)$. The result is

$$B = (2h)^{-1} \exp[\pi(t_U + t_L)(z - z_0)/(2h)]/\{\exp[\pi(z - z_0)/h] - 1\} - [2\pi(z - z_0)]^{-1} \quad (44)$$

$$E = -(2h)^{-1} \exp[\pi(t_U + t_L)(z - z_0{}^*)/(2h) + i\pi(t_U - t_L)/2]/\{\exp[\pi(z - z_0{}^*)/h] + 1\} \quad (45)$$

Using Eq. (40) we then obtain the analytic parts of the influence functions [Eq. (16)]:

$$H_\sigma = B + E$$
$$H_\gamma = i(B - E) \quad (46)$$

Near $z = z_0$, where B has a removable singularity, we may expand Eq. (44) in a power series in $z - z_0$, utilizing Bernoulli polynomials[20] of the argument $(t_U + t_L)/2$. In particular

$$\lim_{z \to z_0} B = (t_U + t_L - 1)/(4h) \quad (47)$$

An interesting property can be demonstrated from the series Eqs. (41) and (42): keeping $|z - z_0|$ finite, and increasing the distance between the walls $h \to \infty$, we find that B and E tend uniformly to zero, and consequently $H_\sigma \to 0$, $H_\gamma \to 0$. Hence, for infinitely distant walls the influence functions [Eq. (16)] reduce to the complex disturbance velocities due to a source and a vortex in free air.

Uniqueness is handled here by a simple contradiction argument. Suppose ϕ is a difference of two regular solutions. From the first Green's identity for a harmonic function ϕ and the inward orientation of n

$$\int_{D_F} |\operatorname{grad} \phi|^2 \, dA = -\int_{C_F} \phi(\partial\phi/\partial n) \, ds + (\lim_{x \to \infty} - \lim_{x \to -\infty}) \int_{-h/2}^{h/2} \phi(\partial\phi/\partial x) \, dy$$

Using $\partial\phi/\partial n = 0$ on C, Eqs. (29) on C_w, and the fact that ϕ decays exponentially in D_F as $|x| \to \infty$ (follows from the separation of variables for ϕ harmonic in a semi-infinite strip), the right-hand side of the above equation is found to be zero. Then $\partial\phi/\partial x = \partial\phi/\partial y = 0$; so it follows that w is unique in D_F.

V. Compressibility Corrections

To extend the present wind tunnel theory to low subsonic Mach numbers M, we can use the familiar corrections based on linearized equation for the disturbance velocity potential

$$\beta^2 \partial^2\tilde{\phi}/\partial\tilde{x}^2 + \partial^2\tilde{\phi}/\partial\tilde{y}^2 = 0 \quad (48)$$

where

$$\beta = (1 - M^2)^{1/2} \quad (49)$$

From the geometrical point of view, the most straightforward approach embodies the *Goethert rule*.[21] Using

$$x = \tilde{x}, \qquad y = \beta\tilde{y} \quad (50)$$

the entire (compressible-flow) plane $\tilde{x}$, $\tilde{y}$ is transformed into the related (incompressible-flow) plane x, y where Eq. (48) reduces to the Laplace equation. From Eq. (50) we have

$$h = \beta\tilde{h} \quad (51)$$

where $\tilde{h}$ is the actual distance between the walls in the $\tilde{x}$, $\tilde{y}$ plane. Assuming the wall boundary condition [Eq. (3)] to be invariant under the compressibility transformation [Eq. (50)], we obtain for the case analyzed in Sec. IV

$$P_U = \tilde{P}_U/\beta, \qquad P_L = \tilde{P}_L/\beta \quad (52)$$

where $\tilde{P}_U$ and $\tilde{P}_L$ are the porosity factors for upper and lower walls in compressible flow. The transformed quantities P_U and P_L, which enter Eqs. (35) and (39), have now only a formal meaning. The problem can then be solved in the x, y plane as described in the previous sections. The corresponding transformation for $\tilde{\phi}$ is derived in conjunction with a thin airfoil: in order to satisfy a thin airfoil approximation of the boundary condition [Eq. (4)] in both $\tilde{x}$, $\tilde{y}$ and x, y planes, we have to set

$$\phi = \beta^2\tilde{\phi} \quad (53)$$

Consequently, the pressure coefficients at corresponding points $\tilde{x}$, $\tilde{y}$ and x, y in the two flows are related by

$$\tilde{C}_p = C_p/\beta^2 \quad (54)$$

where C_p is given by Eq. (28).

The more familiar *Prandtl-Glauert rule*[22] assumes that for an airfoil located near $\tilde{y} = 0$, the flow coordinates are scaled according to Eq. (50), whereas the airfoil remains unchanged.

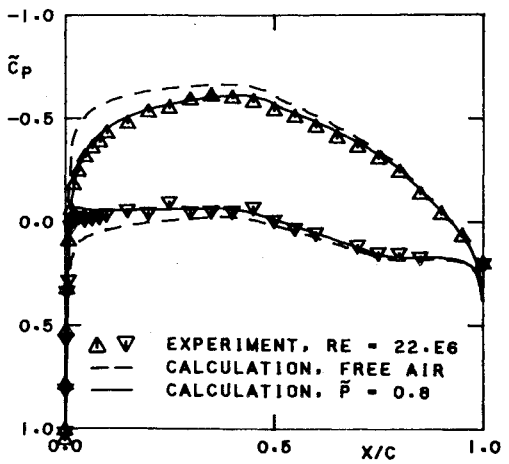

Fig. 5 NACA 64A410 airfoil, 15 in. model, $M = 0.503$, $\alpha = 0.68°$.

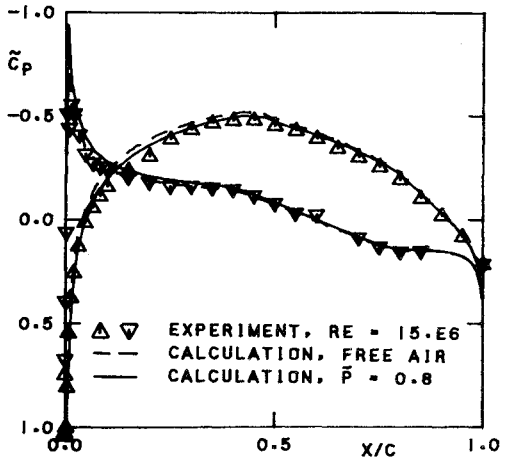

Fig. 7 NACA 64A410 airfoil, 10 in. model, $M = 0.501$, $\alpha = -1.39°$.

Hence, Eqs. (51) and (52) hold as for the Goethert rule. It follows that

$$\phi = \beta\tilde{\phi} \tag{55}$$

and consequently

$$\tilde{C}_p = C_p/\beta \tag{56}$$

The *Kármán-Tsien rule*[23] be applied in the same way as the Prandtl-Glauert rule, except that

$$\tilde{C}_p = C_p/[\beta + (1-\beta)C_p/2] \tag{57}$$

VI. Theoretical and Experimental Results

To illustrate the application of the present method to a perforated wind tunnel, a series of pressure distributions were calculated for a NACA 64A410 airfoil and compared with experimental results. The numerical solution of integral equations of Sec. III was carried out by the finite element technique.[3,4] The airfoil contour was approximated by 65 straight line elements, assuming the values of σ and γ to be constant over each of them. In the treatment of Eq. (25), the discrete values of γ_1 were chosen equal to the distance of the element midpoints from the trailing edge. Having replaced integrations by finite summations, Eqs. (24) and (25) were applied to midpoints z of the elements. The resultant systems of linear algebraic equations in σ_0 and σ_1 were solved by the Gauss elimination method. The computation time used by an IBM 360/67 computer was about 30 sec for one flow case.

The experiments were performed in the NAE 5 ft blowdown wind tunnel using a two-dimensional 15 in. × 60 in. test section, described in Ref. 24. The perforated upper and lower walls were adjusted to have a 6% open area ratio. The pressure measurements on 10 in. and 15 in. models of the NACA 64A410 airfoil section used here, were conducted as a part of an earlier wind tunnel calibration program.[25]

Figures 4–6 show experimental pressure distributions obtained on the 15 in. chord model (airfoil chord/wind tunnel height ratio $c/\tilde{h} = 0.25$) at Mach number $M = 0.5$, Reynolds number based on chord $Re = 22 \times 10^6$, and three angles of attack, measured with respect to the wind tunnel axis: $\alpha = -1.48°$, 0.68°, and 2.25°. The experimental results are compared with corresponding wind tunnel and free air calculations. The porosity factor $\tilde{P} = \tilde{P}_U = \tilde{P}_L = 0.8$ was selected to match the experiment at $\alpha = 0.68°$, Fig. 5. It is seen, however, that good agreement is obtained at all three angles of attack.

In Figs. 7–9, a similar series of tests and calculations is shown for the 10 in. chord model ($c/\tilde{h} = 0.167$). In order to achieve identical freestream conditions at the walls. the tests were performed again at $M = 0.5$, and the same pressure as for the 15 in. model. Consequently, the Reynolds number based on chord was smaller: $Re = 15 \times 10^6$. Using the porosity factor $\tilde{P} = 0.8$, the wind tunnel calculations are again in good agree-

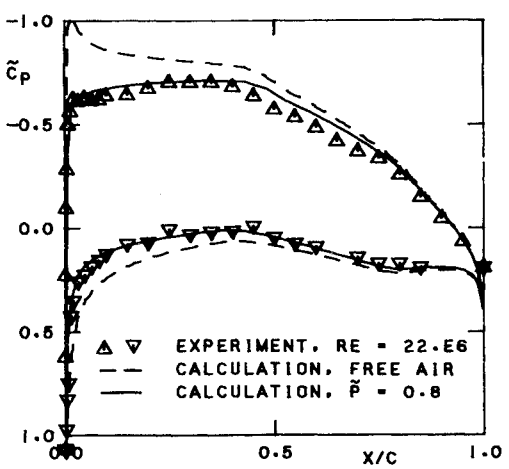

Fig. 6 NACA 64A410 airfoil, 15 in. model, $M = 0.502$, $\alpha = 2.25°$.

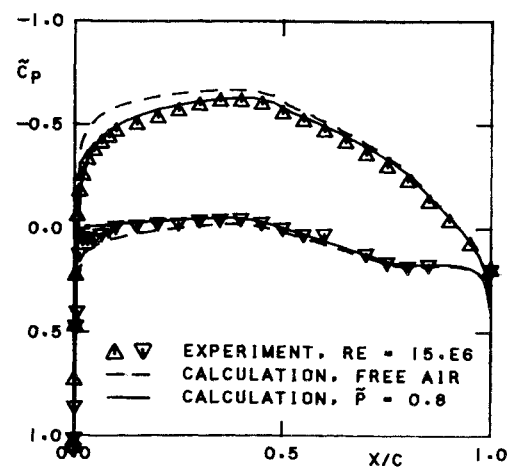

Fig. 8 NACA 64A410 airfoil, 10 in. model, $M = 0.500$, $\alpha = 0.72°$.

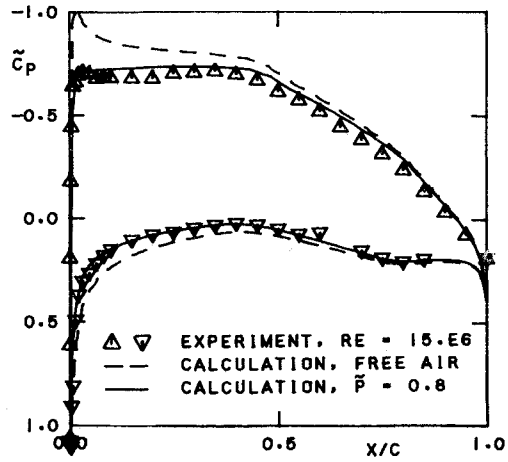

Fig. 9 NACA 64A410 airfoil, 10 in. model, $M = 0.500$, $\alpha = 2.24°$.

ment with the experimental data. As expected, the comparisons with free air calculations clearly indicate that the wind tunnel effect is more pronounced for the 15 in. model. In view of high Reynolds numbers and attached flow conditions the displacement effect of boundary layers is believed to be insignificant, and hence has not been included in the calculations.

All the compressible-flow calculations were worked out with the help of the Prandtl-Glauert rule. Inaccuracies introduced by this simple compressibility transformation can be estimated from free air calculations, where it is also possible to obtain exact solutions, based on nonlinear subsonic theory. Figure 10 compares the free air case of Fig. 5 with the solution by the Sells' inversion method[26] computed according to Refs. 27 and 28. The agreement is seen to be good with the exception of a small region on the upper surface of the airfoil.

VII. Conclusions

A method has been presented for the calculation of subsonic potential flow about two-dimensional airfoils in ventilated wind tunnels. Results obtained by this method at Mach number $M = 0.5$ show very good agreement with wind tunnel measurement on two NACA 64A410 airfoils of different chord lengths.

Due to the generality of the present formulation, the developed procedure can be applied to airfoils of arbitrary shape, size, and locations in the wind tunnel. Specific applications of the present method may include wind tunnel flows past multi-component airfoils[29] and finite cascades of airfoils. The method is believed to become useful in dealing with difficulties involved in the correlation of theory with wind tunnel tests.

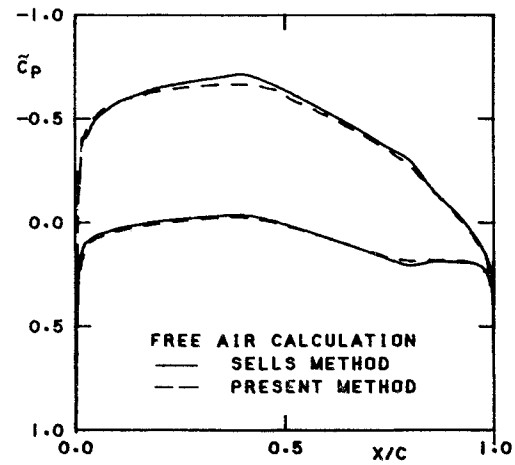

Fig. 10 Comparison of free air calculations for NACA 64A410 airfoil, $M = 0.503$, $\alpha = 0.68°$.

References

[1] Garner, H. C., Rogers, E. W. E., Acum, W. E. A., and Maskell, E. C., "Subsonic Wind Tunnel Wall Corrections," AGARDograph 109, Oct. 1966.

[2] Poincaré, H., *Leçons de Mécanique Céleste*, Vol. 3, Chap. X, Paris, 1910.

[3] Giesing, J. P., "Potential Flow about Two-Dimensional Airfoils," Pt. II, Rept. LB-31946, 1965, Douglas Aircraft Co., Long Beach, Calif.

[4] Hess, J. L. and Smith, A. M. O., "Calculation of Potential Flow about Arbitrary Bodies," *Progress in Aeronautical Sciences*, Vol. 8, 1967, pp. 1–138.

[5] Ebihara, M., "A Study of Subsonic, Two-Dimensional Wall-Interference Effect in a Perforated Wind Tunnel..." TR-252T, Jan. 1972, National Aerospace Lab., Tokyo, Japan.

[6] Prager, W., "Die Druckverteilung an Körpern in ebener Potentialströmung," *Physikal Zeitschrift*, Vol. XXIX, pp. 865–869, 1928.

[7] Martensen, E., "Die Berechnung der Druckverteilung an dicken Gitterprofilen mit Hilfe von Fredholmschen Integralgleichungen zweiter Art," Mitteilungen des Max-Planck-Instituts für Strömungsforschung und der Aerodynamischen Versuchsanstalt Göttingen, No. 23, 1959.

[8] Jacob, K. and Riegels, F. W., "Berechnung der Druckverteilung endlich dicker Profile ohne und mit Klappen und Vorflügeln," *Zeitschrift für Flugwiss.*, Vol. 11, 1963, pp. 357–367.

[9] Muskhelishvili, N. I., *Singular Integral Equations*, Noordhoff, Groningen, The Netherlands, 1953.

[10] Antontsev, S. N., "Subsonic Gas Flows in Multiply-Connected Regions," *Fluid Dynamics Transactions*, Vol. 5, Part II, 1971, pp. 7–18.

[11] Baldwin, B. S., Turner, J. B., and Knechtel, E. D., "Wall Interference in Wind Tunnels with Slotted and Porous Boundaries at Subsonic Speeds," TN-3176, May 1954, NACA.

[12] Parkinson, G. V. and Lim, A. K., "On the Use of Slotted Walls in Two-Dimensional Testing of Low Speed Airfoils," *CASI Transactions*, Vol. 4, No. 2, 1971, pp. 81–87.

[13] Wright, R. H., "The Effectiveness of the Transonic Wind-Tunnel as a Device for Minimizing Tunnel-Boundary Interference for Model Tests at Transonic Speeds," AGARD Rept. 294, March 1959.

[14] Lo, C. F., "Wind-Tunnel Wall Interference Reduction by Streamwise Porosity Distribution," *AIAA Journal*, Vol. 10, No. 4, April 1972, pp. 547–550.

[15] Maeder, P. F. and Wood, A. D., "Transonic Wind Tunnel Test Sections," *Zeitschrift für angewandte Math. u. Phys.*, Vol. 7, 1956, pp. 177–212.

[16] Kassner, R. R., "Subsonic Flow Over a Body Between Porous Walls," TR 52-9, Feb. 1952, Wright Air Development Center, Wright-Patterson Air Force Base, Ohio.

[17] Brescia, R., "Wall Interference in a Perforated Wind Tunnel," TM-1429, May 1957, NACA.

[18] Kacprzynski, J. J., "A Method for Calculation of the Linearized Subcritical Flow past an Arbitrary Airfoil in the Wind Tunnel with Porous Walls," HSA-65, July 1972, National Aeronautical Establishment, NRC, Ottawa, Canada.

[19] Mokry, M., Peake, D. J., and Bowker, A. J., "Wall Interference on Two-Dimensional Supercritical Airfoils, Using Wall Pressure Measurements to Determine the Porosity Factors for Tunnel Floor and Ceiling," LR-575, Feb. 1974, NRC, Ottawa, Canada.

[20] Abramowitz, M. and Stegun, I. A., *Handbook of Mathematical Functions*, National Bureau of Standards, Washington, D.C., June 1964, pp. 804–808.

[21] Gothert, B., "Plane and Three-Dimensional Flow at High Subsonic Speeds," TM-1105, Oct. 1946, NACA.

[22] Glauert, H., "The Effect of Compressibility on the Lift of an Aerofoil," *Proceedings of the Royal Society*, Ser. A., Vol. 118, 1927, pp. 113–119.

[23] von Kármán, T., "Compressibility Effects in Aerodynamics," *Journal of the Aeronautical Sciences*, Vol. 8, July 1941, pp. 337–356.

[24] Ohman, L. H. and Brown, D., "The NAE High Reynolds Number 15″ × 60″ Two-Dimensional Test Facility; Description Operating Experiences and Some Representative Results," AIAA Paper 71-293, Albuquerque, N. Mex., 1971.

[25] Brown, D., Mokry, M., and Ohman, L. H., "Further Calibration of the 15″ × 60″ Two-Dimensional Test Facility with 6% Open Floor and Ceiling at the Test Section," Project Rept. 5 × 5/0050, Sept. 1971, NRC, Ottawa, Canada.

[26] Sells, C. C. L., "Plane Subcritical Flow past a Lifting Airfoil," *Proceedings of the Royal Society*, Series A. 308, 1968, pp. 371–401.

[27] Kacprzynski, J. J., "Fortran IV Program for the Catherall-Foster-Sells Method for Calculation of the Plane Inviscid Incompressible Flow past a Lifting Aerofoil," LTR-HA-2, April 1970, NRC, Ottawa, Canada.

[28] Kacprzynski, J. J., "Fortran IV Program for the Sells Method for Subcritical Two-Dimensional Inviscid Flow Calculations past a Lifting Aerofoil," LTR-HA-3, April 1970, NRC, Ottawa, Canada.

[29] Mokry, M., "Calculation of Flow Past Multi-Component Airfoils in Perforated Wind Tunnel," *Proceedings of the 4th Canadian Congress of Applied Mechanics*, Montreal, May 1973.

JANUARY 1975 AIAA JOURNAL VOL. 13, NO. 1

Comparison of Pressure and LDV Velocity Measurements with Predictions in Transonic Flow

RONALD D. FLACK,* AND H. DOYLE THOMPSON†
Purdue University, West Lafayette, Ind.

This paper presents a comparison of the sonic line location in a series of two-dimensional nozzles as determined by static pressure measurements, Laser Doppler Velocimeter (LDV) velocity measurements, and an analytical solution based on a series expansion. Wall static pressure data have been obtained for 13 different two-dimensional nozzles, including 10 unsymmetrical nozzles. An LDV has been designed, built, and used to make extensive flow velocity measurements in two of the nozzles. The system uses a 4 w argon laser in a forward scatter, dual beam configuration. The analytical solution is based on a series expansion in terms of the wall geometry in the transonic region and is developed for annular as well as two-dimensional inviscid internal flows. The analytical sonic line location is slightly upstream of the experimental sonic line based on static pressure measurements in all thirteen of the nozzles examined. The difference for the nozzles tested is between 1 and 4% (based on Mach number) and is largely attributable to the neglecting of boundary-layer effects in the analytical model. The sonic lines based on LDV measurements fall between the analytical and static pressure sonic lines. The agreement is excellent. The experimental and analytical data confirm that transonic flows may be sensitive to small changes in the flow boundaries, and indicate that the sonic line location in annular nozzles (i.e., plug and forced deflection nozzles), and in unsymmetric two-dimensional nozzles may be very different from the essentially one-dimensional uniform flow that is commonly assumed.

Introduction

TRANSONIC flow has been found to be very dependent on the flow boundaries in that small changes in a flow boundary may dramatically alter the entire flowfield. This nonlinear behavior leads to many interesting problems, not only in the analysis and design of transonic flow passages, but also in the accurate measurement of pressures and velocities in transonic flowfields. There are numerous applications in the fields of jet propulsion, turbomachinery, fluidics, and others. One problem that is partially responsible for the present research is the determination of an accurate supersonic start line in an annular nozzle from which a method of characteristics solution can be initiated. Another application arises in the design and flow analysis in high performance compressors in which the cascades perform as a series of unsymmetric nozzles. Very often a portion of the flowfield is in the transonic range. Although the flow is three-dimensional, the solution for a two-dimensional unsymmetrical transonic flowfield is a useful and important approximation to the actual flow.

Analytically, the problem of internal transonic flow has been examined by several methods. Sauer,[1] Hall,[2] Kleigel and Levine,[3] Levine and Coats,[4] and Moore and Hall[5] have used small perturbation approaches for inviscid nozzles. More recently, Thompson and Flack[6-7] have applied the approach to unsymmetric two-dimensional and annular nozzles. Results from Refs. 6 and 7 are included herein.

Serra[8] and Wehofer and Moger[9] have used asymptotic steady-state solutions to the time-dependent equations to determine the transonic flowfield in two-dimensional and annular axisymmetric nozzles. Brunell[10] used the time-dependent solution for two-dimensional nozzles, and Prozan and Kooker[11] used an error minimization relaxation scheme for axisymmetric nozzles to obtain the steady-state solution. Holt[12] and Liddle and Archer[13] have used the Method of Integral Equations in solving two-dimensional and axisymmetric flow problems. Hopkins and Hill[14,15] implemented an inverse method originally formulated by Friedrichs.[16] The work has been supplemented by the work of Morden and Farquhar[17] and is applicable to conventional and annular nozzles.

Experimentally, only a small amount of data involving internal transonic flow has been published. A major portion of this data is wall-static pressure measurements. Jacobs[18] experiment-

Presented as Paper 74-15 at the AIAA Aerospace Sciences Meeting, Washington, D.C., January 30–February 1, 1974; submitted February 14, 1974; revision received June 28, 1974. This work was sponsored by the U.S. Army Missile Command, Redstone Arsenal, Ala., under Contract DAAH01-72-C-0089.

Index categories: Subsonic and Transonic Flow; Nozzle and Channel Flow.

* Graduate Research Assistant. Student Member AIAA.

† Professor. Member AIAA.